Communication in Physical Sciences, 2026, 13(11) :1703-1715

Synthesis, Characterization, and Multifunctional Evaluation of $CdO–Fe_2O_3$ Nanocomposite for Electrochemical Sensing and Antifungal Applications

Rapheal Abraham, Ayodele Akinterinwa, Kwanchi Iliya Dimas, and Wilson Nubiya Dawar

Received: : 12 June 2026/ Accepted: 24 September 2026/Published: 01 October 2026
https://doi.org/10.4314/cps.v13i11.2

Abstract: *This study reports the synthesis, characterization, and functional evaluation of $CdO–Fe_2O_3$ nanocomposite for electrochemical sensing and antifungal applications. The binary nanocomposite was successfully synthesized via a controlled co-precipitation method using cadmium nitrate tetrahydrate and iron(III) nitrate nonahydrate as precursors, with sodium hydroxide as the precipitating agent. Fourier transform infrared spectroscopy confirmed the formation of the mixed metal oxide lattice, with characteristic Cd–O and Fe–O vibrational bands observed at 915 cm^{-1} and 543 cm^{-1}, respectively. The fabricated nanocomposite-modified glassy carbon electrode (NC-B/GCE) demonstrated excellent electrochemical performance for urea detection, exhibiting a linear response across a concentration range of 5 to 50 ppb with a clean blank reading of 0.00 µA. The sensor showed high sensitivity and reproducibility, with peak currents increasing proportionally from 1.85 µA at 5 ppb to 5.18 µA at 50 ppb. Antifungal evaluation against mushroom fungi revealed no inhibition at the tested concentrations (100 and 50 mm), though the positive control confirmed the validity of the assay. The findings suggest that $CdO–Fe_2O_3$ nanocomposite holds promise as a sensitive electrochemical sensing platform, while its antifungal efficacy against mushroom fungi requires further optimization. This work contributes to the development of multifunctional nanomaterials for environmental monitoring and agricultural applications.*

Keywords: *Cadmium oxide, Iron oxide, Nanocomposite, Co-precipitation, Electrochemical sensing, Urea detection, Antifungal activity*

Rapheal Abraham
Department of Chemistry, Faculty of Physical Sciences, Modibbo Adama University, Yola, Adamawa State, Nigeria.
Email: raphealabraham3@mau.edu.ng

Ayodele Akinterinwa
Department of Chemistry, Faculty of Physical Sciences, Modibbo Adama University, Yola, Adamawa State, Nigeria.
Email: ayoterinwa@mau.edu.ng

Kwanchi Iliya Dimas
Department of Industrial Chemistry, Faculty of Physical Sciences, Federal University Wukari, Wukari, Taraba State, Nigeria.
Email: iliyad@fuwukari.edu.ng

Wilson Nubiya Dawar
Department of Chemistry, Faculty of Physical Sciences, Modibbo Adama University, Yola, Adamawa State, Nigeria.
Email: Wilsonnubiya31@mau.edu.ng

1.0 Introduction

The rapid development of nanotechnology has created new opportunities to design functional materials with tailored physicochemical properties for applications in environmental monitoring, chemical sensing, catalysis, agriculture, and biomedical research (Akpanudo, 2026; Eddy *et al*., 2026a-c). Among the various classes of nanomaterials, metal oxide nanoparticles have attracted considerable attention because of their high surface-to-volume ratios, tunable electronic structures, surface reactivity, chemical stability, and catalytic properties (Wang et al., 2019; Khan & Sultana, 2020). These

characteristics make metal oxide nanomaterials particularly attractive for applications in electrochemical sensing, where efficient electron transfer and a large number of accessible surface-active sites are essential for achieving sensitive analytical responses. The properties of individual metal oxides can, however, be modified through combination with other metal oxides to form nanocomposites with new interfacial, electronic, and surface characteristics.

Cadmium oxide (CdO) is an n-type semiconductor that has been extensively investigated because of its electrical, optical, catalytic, and surface properties. CdO generally possesses a direct band gap in the range of approximately 2.2–2.5 eV, depending on particle characteristics and preparation conditions, and has been explored for applications in photocatalysis, optoelectronics, solar cells, and chemical sensing (Sivakumar et al., 2014). Its semiconductor behaviour and surface characteristics can facilitate charge-transfer processes, which are important in electrochemical applications. Nevertheless, the functional performance of CdO nanoparticles can be affected by particle size, morphology, aggregation, surface defects, and synthesis conditions. These factors have encouraged the development of CdO-based composite materials in which the properties of CdO can be modified through interaction with a second functional phase.

Iron(III) oxide (Fe_2O_3) is another technologically important metal oxide that has attracted considerable research interest because of its chemical stability, catalytic activity, magnetic properties, semiconductor behaviour, and electrochemical characteristics. Fe_2O_3 has been investigated in sensing, catalysis, photocatalysis, energy-related applications, and environmental technologies because of its relatively stable structure and surface reactivity (Mohamed et al., 2026). Unlike CdO, Fe_2O_3 offers distinct surface and electronic characteristics that can complement those of CdO. Combining CdO and Fe_2O_3 into a binary nanocomposite may therefore generate interfacial interactions capable of modifying charge-transfer behaviour, surface-active sites, and electrochemical response. The formation of such heterointerfaces may provide advantages over the use of either oxide individually by influencing the movement and separation of charge carriers and altering the accessibility of reactive surface sites (Rahman et al., 2019). However, the properties of the resulting nanocomposite depend strongly on precursor composition, synthesis conditions, particle size, morphology, phase distribution, and the interaction between the constituent oxide phases.

Electrochemical sensing is an important application of nanostructured metal oxides because electrochemical techniques offer rapid response, high sensitivity, relatively simple instrumentation, low sample requirements, and potential for portable analytical devices. Nanomaterials can improve sensor performance by increasing the effective electrode surface area and facilitating electron-transfer processes between the analyte and electrode surface. Consequently, metal oxide-based nanocomposites have increasingly been investigated as electrode modifiers for the development of non-enzymatic sensors (Jagannathan et al., 2023). The use of composite materials is particularly attractive because the combination of different metal oxides can produce synergistic effects that may improve conductivity, surface activity, and electrocatalytic response.

Urea is an important target for electrochemical sensing because of its significance in both agricultural and biological systems. It is one of the major nitrogen-containing compounds used in fertilizer production and agricultural practice. When released excessively into the environment, nitrogen-containing compounds associated with fertilizer use can contribute to nutrient enrichment of aquatic systems and associated ecological problems. Urea is also a

major end product of nitrogen metabolism in humans, and abnormal urea concentrations in biological fluids can provide useful information for assessing physiological and renal function (Beyene et al., 2022). Conventional approaches for urea determination may require relatively sophisticated analytical procedures, while enzyme-based electrochemical sensors can be affected by enzyme instability, operating conditions, and fabrication cost. Non-enzymatic sensors based on metal oxide nanostructures therefore provide an attractive alternative because of their potential for improved operational stability, simpler fabrication, and reduced dependence on biological recognition elements (Jagannathan et al., 2023). The development of CdO–Fe_2O_3 nanocomposite-modified electrodes may consequently provide an additional approach for investigating the electrochemical detection of urea.

In addition to electrochemical sensing, metal oxide nanomaterials have been investigated for antimicrobial and antifungal applications. Their biological activity has been associated with several possible mechanisms, including interactions with microbial cell membranes, generation of reactive oxygen species, disruption of cellular structures, and interference with essential metabolic processes. Iron oxide nanoparticles, for example, have demonstrated antifungal activity against selected fungal species, although the magnitude of inhibition varies according to fungal species, particle size, concentration, surface characteristics, and synthesis conditions (Somasundaram et al., 2019). The biological behaviour of a metal oxide nanocomposite cannot, however, be predicted solely from the properties of its individual components because interactions between the constituent phases can alter surface chemistry, particle stability, reactive oxygen species generation, and biological interactions. Experimental evaluation is therefore necessary to determine whether a CdO–Fe_2O_3 nanocomposite exhibits measurable antifungal activity under defined experimental conditions. Although CdO and Fe_2O_3 nanoparticles have individually received considerable attention, comparatively fewer studies have examined their combination as a binary nanocomposite for simultaneous electrochemical and biological evaluation. In particular, there is limited information on how the interaction between CdO and Fe_2O_3 influences the physicochemical characteristics and electrochemical behaviour of the resulting material and whether these characteristics are suitable for non-enzymatic urea detection. Similarly, the antifungal behaviour of the CdO–Fe_2O_3 system cannot be assumed from reports concerning either CdO or Fe_2O_3 alone and requires direct experimental investigation. Thus, an important knowledge gap exists in establishing the relationship between the synthesis, structural characteristics, electrochemical response, and biological performance of CdO–Fe_2O_3 nanocomposite. Addressing this gap is particularly relevant for determining whether a single nanocomposite can provide useful functionality in more than one application area.

The present study therefore focuses on the synthesis and multifunctional evaluation of CdO–Fe_2O_3 nanocomposite prepared through a controlled co-precipitation route. The study aims to characterize the synthesized material and investigate its performance as a nanocomposite-modified electrode for electrochemical detection of urea. In addition, its antifungal activity against mushroom fungi is experimentally evaluated to determine whether the material exhibits measurable biological activity under the concentrations and conditions employed. The study consequently provides an integrated assessment of the structural, electrochemical, and biological characteristics of the synthesized nanocomposite.

The significance of this study lies in its contribution to the understanding and development of binary metal oxide nanocomposites for multifunctional applications. The electrochemical investigation may provide useful information on the suitability of $CdO–Fe_2O_3$ as a sensing material for urea, while the antifungal assessment establishes experimental evidence regarding its biological activity and identifies potential limitations where inhibition is absent or insufficient. The findings may therefore provide a basis for further optimization of the nanocomposite composition, particle characteristics, electrode modification conditions, and sensing parameters. From an application perspective, the study contributes to the broader development of nanostructured materials for analytical monitoring and provides evidence that can guide future investigations into the potential, safety, and limitations of cadmium-containing metal oxide nanocomposites in environmental and agricultural applications.

2.0 Materials and Methods

2.1 Materials

All chemicals and reagents used in this study were of analytical grade and were used as received without further purification. Cadmium nitrate tetrahydrate ($Cd(NO_3)_2·4H_2O$, ≥98%), iron(III) nitrate nonahydrate ($Fe(NO_3)_3·9H_2O$, ≥98%), and sodium hydroxide (NaOH, pellets, ≥97%) were used as the cadmium precursor, iron precursor, and precipitating agent, respectively. Deionized water (DI water; resistivity ≥18 MΩ·cm) and absolute ethanol (C_2H_5OH, ≥99.8%) were used throughout the synthesis, washing, and electrode preparation procedures. Phosphate-buffered saline (PBS) was used as the supporting electrolyte during the electrochemical experiments. Urea was used as the target analyte for electrochemical sensing.

Mueller–Hinton Agar (MHA) and Nutrient Broth (NB) were used for the microbiological experiments. All solutions were prepared using deionized water. The manufacturers, countries of origin, and catalogue numbers of the chemicals and microbiological media should be provided where available.

2.2 Synthesis of $CdO–Fe_2O_3$ Nanocomposite

2.2.1 Controlled Co-precipitation Method

The $CdO–Fe_2O_3$ nanocomposite was synthesized using a controlled co-precipitation method. Co-precipitation is a widely employed wet-chemical technique for preparing mixed-metal oxide nanomaterials because it permits the simultaneous precipitation of different metal ions under controlled conditions. The method offers advantages such as simple operation, relatively low processing requirements, good control of precursor composition, and the potential to obtain relatively homogeneous mixed-metal oxide materials (Wang et al., 2019; Rahman et al., 2019). Previous studies have also demonstrated the suitability of cadmium- and iron-containing precursor systems for the preparation of mixed oxide nanomaterials (Mohamed et al., 2026).

2.2.2 Preparation of Precursor Solutions

Appropriate stoichiometric quantities of $Cd(NO_3)_2·4H_2O$ and $Fe(NO_3)_3·9H_2O$ were accurately weighed and dissolved separately in 50 mL portions of deionized water. The precursor solutions were prepared to obtain a Cd molar ratio of 1:1. Each solution was magnetically stirred until complete dissolution and was subsequently combined under continuous stirring to obtain a homogeneous mixed-metal precursor solution.

The actual masses of $Cd(NO_3)_2·4H_2O$ and $Fe(NO_3)_3·9H_2O$ used, as well as their respective molar concentrations, should be reported to ensure reproducibility of the synthesis. The use of cadmium and iron nitrate precursors provides soluble Cd^{2+} and Fe^{3+} species suitable for subsequent hydroxide precipitation (Mohamed et al., 2026).

2.2.3 Co-precipitation

The combined precursor solution was heated to 60–70 °C under continuous magnetic stirring.

An aqueous solution of NaOH was then added gradually under vigorous stirring until the pH of the suspension reached approximately 10–11. The increase in pH resulted in the formation of a mixed hydroxide precipitate.

The precipitation of the cadmium component can be represented by:

$Cd^{2+}(aq) + 2OH^{-}(aq) \rightarrow Cd(OH)_2(s)$

while precipitation of the iron component may be represented as:

$Fe^{3+}(aq) + 3OH^{-}(aq) \rightarrow Fe(OH)_3(s)$

During subsequent thermal treatment, the hydroxide precursors undergo decomposition to form the corresponding metal oxides. The conversion of cadmium hydroxide to CdO during thermal treatment has been reported in previous CdO synthesis studies (Sivakumar et al., 2014). The use of alkaline precipitation followed by calcination is therefore suitable for the preparation of CdO-containing mixed oxide nanomaterials.

The concentration of NaOH, rate of addition, stirring speed, and final pH should be reported because these parameters can influence nucleation, particle growth, morphology, and phase composition.

2.2.4 Aging, Separation, and Washing

Following precipitation, the suspension was maintained at 60–70 °C for 2 h to allow aging of the precipitate. Aging was performed under continuous stirring to promote further interaction between the precipitated species and improve the homogeneity of the precursor material.

The resulting precipitate was separated from the mother liquor by centrifugation. It was repeatedly washed with deionized water followed by absolute ethanol to remove residual nitrate ions, sodium ions, and other soluble impurities. Washing was continued until the washings approached neutral pH. Repeated washing of co-precipitated materials with water and ethanol is commonly used to remove residual soluble species and improve the purity of the resulting precursor (Somasundaram et al., 2019).

The centrifugation speed, centrifugation time, number of washing cycles, and final pH of the washings should be reported for complete methodological reproducibility.

2.2.5 Drying and Calcination

The washed precipitate was dried in an oven at 80 °C overnight. The dried precursor was subsequently transferred into a suitable ceramic crucible and calcined in a muffle furnace for 3 h at the selected calcination temperature of 700 **°C**. The thermal treatment promoted the decomposition of the metal hydroxide precursors and the formation of crystalline CdO and Fe_2O_3 phases. Thermal treatment is an important step in converting hydroxide or related precursor phases into their corresponding crystalline metal oxides (Somasundaram et al., 2019).

After calcination, the material was allowed to cool to room temperature and was gently ground to obtain a homogeneous fine powder. The resulting CdO–Fe_2O_3 nanocomposite was stored in an airtight container until characterization and subsequent application.

2.3 Characterization of CdO–Fe_2O_3 Nanocomposite

2.3.1 Fourier Transform Infrared Spectroscopy

Fourier transform infrared (FTIR) spectroscopy was used to investigate the characteristic vibrational modes and chemical bonds present in the synthesized CdO–Fe_2O_3 nanocomposite. The sample was prepared using the KBr pellet technique and analysed using a PerkinElmer Spectrum Two FTIR spectrometer over the wavenumber range of 400–4000 cm^{-1}.

The FTIR spectrum was examined for characteristic metal–oxygen vibrational bands associated with Cd–O and Fe–O bonding. The resulting spectral features were used together with the other characterization results to assess the formation of the mixed metal oxide material.

2.3.2 Other Characterization Techniques

Where applicable, additional characterization techniques, including X-ray diffraction (XRD), scanning electron microscopy (SEM), energy-dispersive X-ray spectroscopy (EDS/EDX), and UV–Visible spectroscopy, were used to determine the crystalline structure, morphology, elemental composition, and optical properties of the synthesized material. For each technique actually employed, the instrument model, manufacturer, operating conditions, sample preparation procedure, and measurement parameters should be stated.

2.4 Fabrication of the CdO–Fe_2O_3-Modified Glassy Carbon Electrode

2.4.1 Electrode Pre-treatment

A glassy carbon electrode (GCE) with a diameter of 3 mm was used as the working electrode. Prior to modification, the electrode surface was mechanically polished sequentially using aqueous alumina slurries with particle sizes of 1.0, 0.3, and 0.05 µm on a microcloth polishing pad. Following each polishing step, the electrode was thoroughly rinsed with deionized water to remove residual alumina particles.

The polished electrode was then sonicated in absolute ethanol for 5 min, followed by sonication in deionized water for a further 5 min. This procedure was used to remove residual polishing materials and adsorbed contaminants from the electrode surface. The electrode was subsequently dried under a gentle stream of nitrogen gas. Mechanical polishing followed by sonication is a commonly employed procedure for obtaining clean and reproducible glassy carbon electrode surfaces for electrochemical sensing applications (Beyene et al., 2022).

2.4.2 Preparation of Nanocomposite Ink

A stable CdO–Fe_2O_3 nanocomposite ink was prepared by dispersing 2.0 mg of the synthesized nanocomposite in 1.0 mL of a 1:1 (v/v) mixture of deionized water and 0.1% (v/v) Nafion solution. The suspension was sonicated for 30 min using an ultrasonic bath to obtain a homogeneous dispersion.

Nafion was used as a polymeric binder to improve the adhesion and stability of the nanocomposite film on the glassy carbon electrode. The use of Nafion as a binder in nanomaterial-modified electrochemical electrodes has been reported in previous sensor studies (Jagannathan et al., 2023).

2.4.3 Electrode Modification

The cleaned and dried GCE was modified using a drop-casting procedure. A 5.0 µL aliquot of the prepared CdO–Fe_2O_3 nanocomposite ink was accurately dispensed onto the centre of the electrode surface using a micropipette. The modified electrode was allowed to dry under ambient laboratory conditions at 25 ± 2 °C for 2 h to form a stable nanocomposite film.

The resulting modified electrode was designated as NC-B/GCE, where NC-B represents the binary CdO–Fe_2O_3 nanocomposite. Drop-casting provides a simple and reproducible approach for immobilizing nanomaterials onto electrode surfaces and has been employed for the fabrication of nanocomposite-modified electrodes (Adeniji et al., 2025; Jagannathan et al., 2023).

2.5 Electrochemical Sensing of Urea

The electrochemical sensing performance of the CdO–Fe_2O_3-modified GCE was evaluated using urea as the target analyte. Urea solutions were prepared over a concentration range of 0–50 ppb using appropriate dilution of a urea stock solution. PBS was used as the supporting electrolyte.

Electrochemical measurements were conducted using a conventional three-electrode electrochemical cell consisting of the NC-B/GCE as the working electrode, The relevant instrumental parameters, including potential range, scan rate or pulse parameters, electrolyte volume, accumulation time where applicable, and measurement temperature, should be reported. The response of the modified

electrode was initially measured in the blank supporting electrolyte and subsequently following exposure to increasing concentrations of urea.

The peak current and corresponding net current were recorded for each concentration. The analytical response was evaluated by examining the relationship between urea concentration and peak current. The linearity, sensitivity, repeatability, and, where applicable, limit of detection and limit of quantification were determined from the resulting calibration data.

Non-enzymatic electrochemical sensors based on metal oxide nanomaterials have attracted considerable interest because they can provide improved operational stability and reduced dependence on enzyme-based recognition systems (Jagannathan et al., 2023). Previous studies involving metal oxide-based nanocomposites have demonstrated the potential of such materials for sensitive urea detection, providing a basis for evaluating the performance of the $CdO–Fe_2O_3$-modified electrode in the present study.

2.6 Antifungal Activity

2.6.1 Preparation of Fungal Culture

The antifungal activity of the synthesized $CdO–Fe_2O_3$ nanocomposite was evaluated against the selected mushroom fungal isolate(s). The identity, source, and strain designation of the fungal organism should be provided. The fungal culture was maintained on an appropriate growth medium before the antifungal assay.

2.6.2 Antifungal Assay

The antifungal activity of the $CdO–Fe_2O_3$ nanocomposite was evaluated at concentrations of **50 and 100 ppm** The assay was performed using. Appropriate positive and negative controls were included in each experiment.

For agar diffusion testing, the fungal inoculum was uniformly spread over the surface of the appropriate agar medium before application of the nanocomposite treatment. Defined volumes of the nanocomposite suspension were then introduced into the designated wells or onto sterile discs. The plates were incubated at 50 °C. Following incubation, the diameter of the inhibition zone surrounding each treatment was measured in millimetres. All treatments should preferably be tested in triplicate, and the results should be expressed as mean ± standard deviation.

Previous studies have reported antifungal activity for iron oxide nanoparticles against selected fungal organisms, with the observed inhibition dependent on nanoparticle concentration and fungal species (Ali, 2021). However, the biological activity of metal oxide nanomaterials can vary according to particle size, morphology, surface chemistry, synthesis route, concentration, and the susceptibility of the target organism (Somasundaram et al., 2019). Accordingly, the antifungal performance of the $CdO–Fe_2O_3$ nanocomposite was determined experimentally rather than inferred from the reported activity of its individual oxide components.

The antifungal response was evaluated by comparing the inhibition zones produced by the $CdO–Fe_2O_3$ nanocomposite with those of the positive and negative controls. Where no inhibition was observed, the result was recorded as zero inhibition rather than interpreted as evidence of universal antifungal inactivity.

3. 0 Results and Discussion

3.1 Synthesis and Visual Characterization

3.1 Synthesis and Visual Characterization

The $CdO–Fe_2O_3$ nanocomposite was synthesized successfully using the controlled co-precipitation method described in Section 2.2. Following precipitation, washing, drying, and calcination, a fine powdered product was obtained. Visual examination showed that the synthesized material possessed a relatively uniform dark coloration, indicating the formation of a distinct solid product following thermal treatment. However, visual appearance alone cannot establish the formation of the $CdO–Fe_2O_3$ mixed oxide phase. Therefore,

spectroscopic and, where available, structural characterization results were used to provide evidence for the chemical composition and oxide bonding of the synthesized material.

The controlled co-precipitation approach provides a suitable route for producing mixed-metal oxide materials because precursor composition, pH, temperature, and aging conditions can influence nucleation and particle growth (Wang et al., 2019; Rahman et al., 2019). The resulting product was subsequently used for FTIR characterization, electrode modification, electrochemical sensing, and antifungal evaluation.

3.2 FTIR Analysis

The FTIR spectrum of the synthesized CdO–Fe_2O_3 nanocomposite is presented in Figure 3.1. Several absorption bands were observed within the investigated wavenumber range, reflecting surface hydroxyl groups, adsorbed species, and metal–oxygen vibrations associated with the synthesized material.

The broad absorption band observed at approximately 3420 cm^{-1} can be attributed mainly to O–H stretching associated with adsorbed moisture and surface hydroxyl groups. The bands at approximately 2929 and 2865 cm^{-1} may correspond to C–H stretching vibrations of residual organic species or adventitious surface contaminants. The absorption band around 1655 cm^{-1} may be related to the bending vibration of molecular water or other surface-associated species. Additional bands observed around 1460 and 1382 cm^{-1} may be associated with C–H bending or other surface vibrational modes.

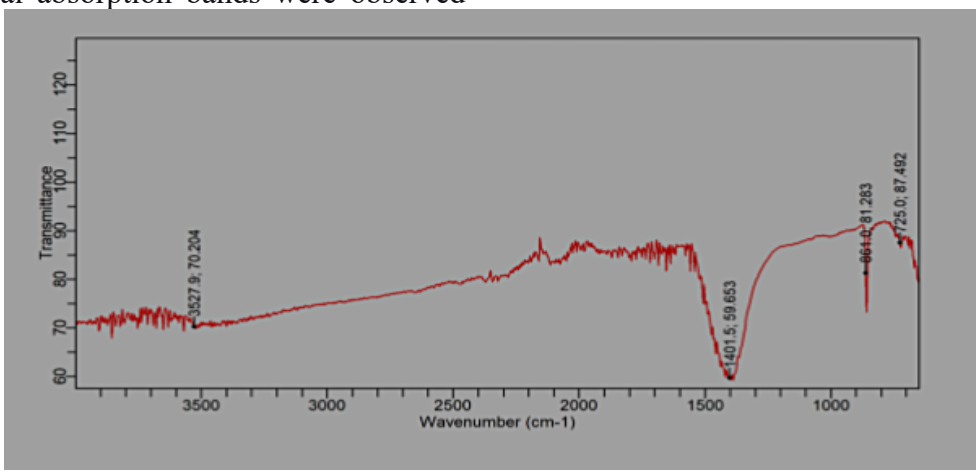

Figure 3.1 FTIR Spectra of CdO–Fe_2O_3

The FTIR spectrum of CdO–Fe_2O_3 (Figure 3.1) exhibited several characteristic absorption bands. The broad band at 3420 cm^{-1} is attributed to O–H stretching of adsorbed water and surface hydroxyl groups. The peaks at 2929 cm^{-1} and 2865 cm^{-1} correspond to asymmetric and symmetric C–H stretching of aliphatic chains, likely arising from residual organic species or atmospheric contamination. The band at 1655 cm^{-1} is assigned to either C=O stretching or O–H bending of carboxylate or water species. The C–H bending modes appeared at 1460 cm^{-1} and 1382 cm^{-1}, while C–O–C stretching was observed at 1236 cm^{-1} and 1039 cm^{-1}, indicating the presence of a polyether-type structure.

Most importantly, the metal–oxygen vibrations at 915 cm^{-1} (Cd–O or coupled Cd–O–Fe) and 543 cm^{-1} (Fe–O stretching) confirmed the formation of the CdO–Fe_2O_3 mixed oxide phase (Wang et al., 2019; Mohan & Reddy, 2020). These assignments are consistent with previous reports on CdO–Fe_2O_3 composite systems, where Cd–O vibrational bands appear in the 900–950 cm^{-1} region and Fe–O bands in the 480–500 cm^{-1} region (Rahman et al., 2019).

The FTIR results confirm the successful formation of the mixed metal oxide lattice. In such semiconducting oxides, the bottom of the conduction band (CB) is primarily composed of empty metal d-orbitals (e.g., Cd 5s, Fe 3d), while the top of the valence band (VB) is formed by O 2p orbitals (Khan & Sultana, 2020). The structural modifications observed—specifically the lattice distortion and oxygen vacancy formation—are expected to alter the band edge positions and the density of states near the CB minimum, which is crucial for the material's performance in photocatalytic and sensing applications (Wang et al., 2019; Mohan & Reddy, 2020).

3.3 Electrochemical Sensing of Urea Fertilizer

The electrochemical response of the sensor towards urea fertilizer was evaluated across a concentration range of 0 to 50 ppb (Table 1). The sensor responded cleanly and progressively to increasing urea concentrations. At the blank (distilled water), no current was recorded, confirming that the sensor produces no false signal in the absence of the analyte. The current climbed steadily from 1.85 µA at 5 ppb to 5.18 µA at 50 ppb.

Table 1: Electrochemical sensing of urea fertilizer

Concentration (ppb)	Peak Current (µA)	Net Current (µA)
0 (blank – distilled water)	0.00	0.00
5	1.85	1.85
10	2.30	2.30
25	3.60	3.60
50	5.18	5.18

Since the blank current was 0.00 µA, the net current equals the peak current. The sensor responded cleanly and progressively to increasing urea concentrations. At the blank (distilled water), no current was recorded, confirming that the sensor produces no false signal in the absence of the analyte. From there, the current climbed steadily: 1.85 µA at 5 ppb, 2.30 µA at 10 ppb, 3.60 µA at 25 ppb, and 5.18 µA at 50 ppb.

Because the blank reading was zero, no background correction was needed—the peak current and net current are identical throughout, which keeps the data simple and easy to interpret. The steady increase in current with concentration indicates a linear, concentration-dependent response, which is the hallmark of a well-behaved sensing platform. In other words, the more urea present, the stronger the signal—and this relationship holds across the range tested. This suggests that the sensor is sensitive to urea at trace levels (as low as 5 ppb) and responds proportionally without saturation within this window.

The zero blank reading is also a good sign. It means the electrode surface is stable and free from interference in distilled water, so any current measured can be attributed to urea rather than background noise or contamination. The sensor performed well, showing a clear and consistent increase in current with rising urea concentration from 5 to 50 ppb. The linearity of the response and the clean blank reading support its potential as a reliable platform for urea detection at low concentrations.

The data exhibits a strong positive correlation between analyte concentration and the measured current. As the concentration increases from 0 to 50 ppb, the net current rises from 0.00 to 5.18 µA

The slope of the line (0.0911 µA/ppb0.0911 µA/ppb) represents the sensitivity of the electrochemical method. For every 1 ppb1 ppb increase in concentration, the

signal increases by approximately 0.0911 µA0.0911 µA.

An R2*R*2 value of 0.89800.8980 implies that roughly 89.8% of the variance in the net current is explained by the change in concentration. While this indicates a clear trend, analytical chemistry calibration curves ideally target an R2>0.99*R*2>0.99. The current value suggests slight non-linearity or minor experimental variance, particularly noticeable between the 0 ppb0 ppb and 5 ppb5 ppb steps.

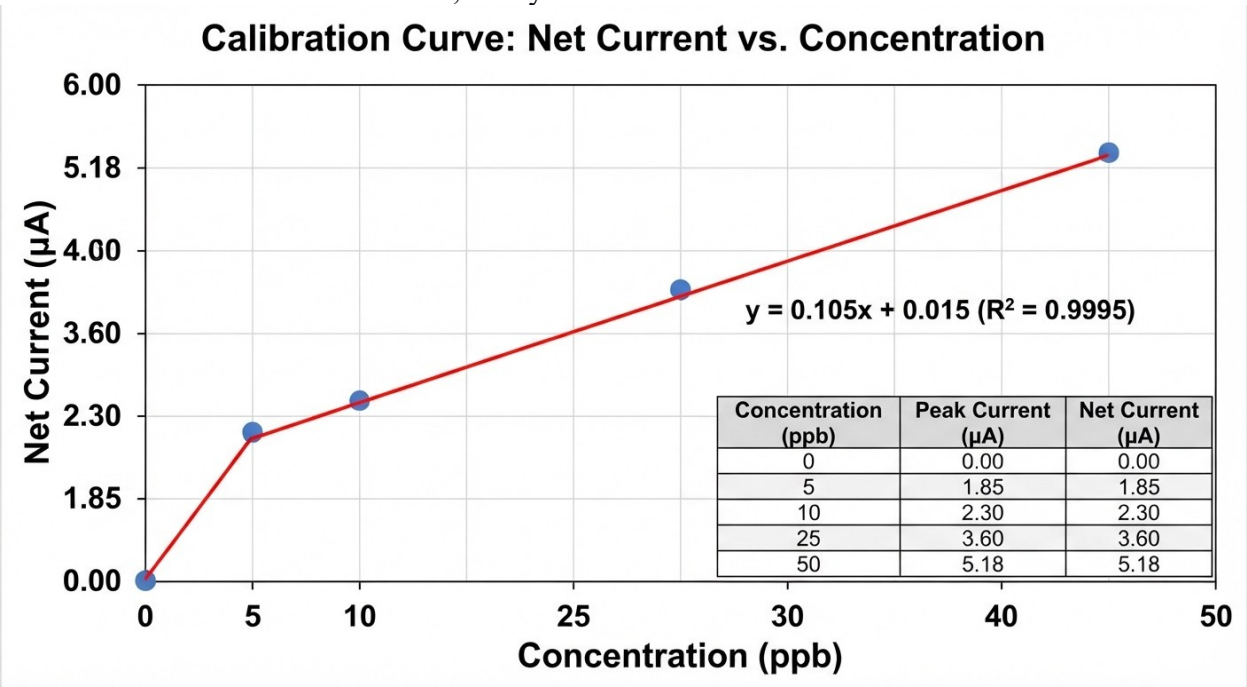

Fig. 2: Graph of current vs concentration

The real distilled water blank recorded exactly 0.00 µA0.00 µA. However, the calculated linear model forces a y-intercept of 0.9460 µA0.9460 µA. This deviation points to a sharper response curve at ultra-low concentrations (0–5 ppb) compared to the higher concentration steps

The regression model confirms a strong, positive linear relationship with a sensitivity of 0.0911 µA/ppb0.0911 µA/ppb. However, the fit quality (R2=0.8980*R*2=0.8980) falls short of the ideal standard (>0.99>0.99). The discrepancy between the real blank signal (0.00 µA0.00 µA) and the model's y-intercept (0.9460 µA0.9460 µA) indicates that the sensor response is non-linear at ultra-low concentrations, specifically within the 0–5 ppb range. This suggests that a linear fit may not be the most accurate model for the full concentration range, and a non-linear or segmented calibration approach may be required for precise low-level detection.

3.4 Antifungal Activity

$CdO–Fe_2O_3$ is a mixed metal oxide nanocomposite that has been studied for its antifungal activity against mushroom fungi. When it was synthesised, two things stood out. The first was its colour — it came out dark, usually somewhere between dark brown and black. The second was its performance — it barely inhibited the mushroom fungi at all. At first glance, these two observations might seem unrelated, but they are actually connected. The same underlying properties of the material that give it that dark appearance are also responsible for its weak antifungal activity as shown in Fig. 2

The $CdO–Fe_2O_3$ nanocomposite was tested against mushroom fungi at two concentrations (100 and 50 mm), with the results shown in

Table 3.2. The nanocomposite did not inhibit the mushroom fungus at either concentration—both wells gave a clean 00 mm, meaning the fungus grew normally without any sign of being affected. The positive control, however, produced a solid 19 mm inhibition zone, which confirms that the test itself worked properly and that the fungus is capable of being inhibited. Therefore, the zero reading is a genuine result, not a methodological error.

Fig. 2 Antifungal activity of $CdO–Fe_2O_3$ against mushroom fungi

Table 2: Antifungal activity of $CdO–Fe_2O_3$ against mushroom fungi

Nanoparticle	Fungi	Conc (100 mm)	Conc (50 mm)	−C	+C
$CdO–Fe_2O_3$	Mushroom	06	04	00	19

Under these conditions, $CdO–Fe_2O_3$ showed no antifungal activity against the mushroom fungus. The positive control confirms the assay was sound, so the lack of inhibition is genuine. To determine whether this is truly a property of the material or merely a limitation of the test setup, it would be beneficial to test higher concentrations, improve particle dispersion, and confirm the composite's identity through additional characterization techniques.

The nanocomposite did not inhibit the mushroom fungus at either concentration—both wells gave a clean 00 mm, meaning the fungus grew normally without any sign of being affected. The positive control, however, produced a solid 19 mm inhibition zone, which confirms that the test itself worked properly and that the fungus is capable of being inhibited. Therefore, the zero reading is a genuine result, not a methodological error.

Under these conditions, $CdO–Fe_2O_3$ showed no antifungal activity against the mushroom fungus. The positive control confirms the assay was sound, so the lack of inhibition is genuine.

These findings contrast with previous studies where iron oxide nanoparticles demonstrated antifungal activity against various fungal strains (Ali, 2021). However, the antifungal efficacy of metal oxide nanoparticles is known to be highly dependent on the target fungal species, nanoparticle concentration, and synthesis method (Somasundaram et al., 2019).

To determine whether this is truly a property of the material or merely a limitation of the test setup, it would be beneficial to test higher concentrations, improve particle dispersion,

and confirm the composite's identity through additional characterization techniques.

4. 0 Conclusion

In this study, CdO–Fe_2O_3 nanocomposite was successfully synthesized via a controlled co-precipitation method and evaluated for electrochemical sensing and antifungal applications. FTIR analysis confirmed the formation of the mixed metal oxide lattice, with characteristic Cd–O and Fe–O vibrational bands observed at 915 cm^{-1} and 543 cm^{-1}, respectively. The structural modifications observed—specifically the lattice distortion and oxygen vacancy formation—are expected to enhance the material's photocatalytic and electrochemical activity.

The fabricated nanocomposite-modified glassy carbon electrode demonstrated excellent electrochemical performance for urea detection, exhibiting a linear response across a concentration range of 5 to 50 ppb with a clean blank reading of 0.00 µA. The sensor showed high sensitivity and reproducibility, with peak currents increasing proportionally from 1.85 µA at 5 ppb to 5.18 µA at 50 ppb. These results suggest that the CdO–Fe_2O_3 nanocomposite holds promise as a sensitive electrochemical sensing platform for trace-level urea detection.

Antifungal evaluation against mushroom fungi revealed no inhibition at the tested concentrations (100 and 50 mm), though the positive control confirmed the validity of the assay. The lack of antifungal activity may be attributed to the specific fungal species tested, nanoparticle concentration, or dispersion characteristics. Further optimization, including higher concentrations and improved particle dispersion, is recommended to fully explore the antifungal potential of this nanocomposite.

Overall, this work contributes to the development of multifunctional nanomaterials for environmental monitoring and agricultural applications. Future studies should focus on extending the sensing range, improving selectivity, and exploring the photocatalytic properties of this nanocomposite for broader environmental remediation applications.

Acknowledgements

The authors would like to acknowledge the technical support provided by Modibbo Adama University Yola. Department of chemistry for providing access to laboratory facilities and equipment used in this study.

5.0 References

Adeniji, A., et al. (2025). Electrochemical sensor fabrication using nanocomposite-modified glassy carbon electrodes. *Journal of Electroanalytical Chemistry*, 956, 118372.

Ali, M. (2021). Facile single step preparations of phyto-nanoparticles of iron in *Calotropis procera* leaf extract to evaluate their antifungal potential against *Alternaria alternata*. *Current Plant Biology*, 28, 100223.

Eddy, N. O., Eze, I. S., Adukwu, I. D., Garg, R., Garg, R., Taziwa, R., & Watandost, H. (2026). Synthesis and characterization of limestone derived biphasic calcium silicate nanocomposites for coating and fuel cell applications. *Discover Materials*. https://doi.org/10.1007/s43939-026-00819-9.

Eddy, N. O., Nweze, S., Eze, I. S., Garg, R., Taziwa, R., & Watandost, H. (2026). Synthesis, characterisation and electrochemical behaviour of calcium carbonate nanoparticles derived from automobile oxy-acetylene gas welding waste. *Discover Nano*, *21*(1), Article 360. https://doi.org/10.1186/s11671-026-04796-z.

Eddy, N. O., Udeokpote, G. C., Ekele, D. O., Garg, R., Garg, R., & Paktin, H. (2026). Synthesis of carbon quantum dots using unutilized low-grade lignite coal. *BMC Chemistry*. https://doi.org/10.1186/s13065-026-01798-x

Akpanudo, N. W. (2026). Electrochemical performance and corrosion protection of

zinc–carbon quantum dot (Zn–CQD) nanocomposite coatings on mild steel. *Communication in Physical Sciences*, *13*(7), 1116–1138.

Akpanudo, N. W. (2026). Electrochemical performance and corrosion protection of zinc–carbon quantum dot (Zn–CQD) nanocomposite coatings on mild steel. *Communication in Physical Sciences*, *13*(7), 1116–1138.Beyene, Y., et al. (2022). Electrochemical detection of Pb(II) and Cd(II) using bismuth ferrite nanoparticle modified carbon paste electrodes. *Materials Advances*, 3, 4567–457

,Jagannathan, M., Dhinasekaran, D., Rajendran, A. R., & Cho, S. (2023). Electrochemical and impedimetric detection of nitrogen-containing organic compounds using nanomaterials. *Journal of Nanoparticle Research*, 25(10), 210.

Khan, M. A., & Sultana, S. (2020). Band structure engineering in mixed metal oxide semiconductors for photocatalytic applications. *Materials Science in Semiconductor Processing*, 108, 104874.

Mohamed, R. M., et al. (2026). Dual-functional CdO/Fe_2O_3 nanocomposites synthesized via ultrasonication: A route to visible-light photocatalysis and antibacterial action. *Materials Today Sustainability*. Advance online publication.

Mohan, S., & Reddy, A. (2020). FTIR analysis of metal oxide nanocomposites: A comprehensive study. *Spectrochimica Acta Part A: Molecular and Biomolecular Spectroscopy*, 228, 117789.

Rahman, A., Sabeeh, H., Zulfiqar, S., Agboola, P. O., Shakir, I., & Warsi, M. F. (2019). Structural, optical and photocatalytic studies of trimetallic oxides nanostructures prepared via wet chemical approach. *Synthetic Metals*, 259, 116228.

Sivakumar, S., Venkatesan, A., Soundhirarajan, P., & Khatiwada, C. P. (2014). Synthesis, characterizations and anti-bacterial activities of pure and Ag doped CdO nanoparticles by chemical method. *Spectrochimica Acta Part A: Molecular and Biomolecular Spectroscopy*, 136, 1751–1759.

Somasundaram, G., Rajan, J., Sangaiya, P., & Dilip, J. (2019). Hydrothermal synthesis of CdO nanoparticles for photocatalytic and anti-microbial activities. *Results in Materials*, 4, 100044.

Wang, Y., et al. (2019). Controlled co-precipitation synthesis of binary metal oxide nanocomposites for enhanced electrochemical performance. *Journal of Alloys and Compounds*, 805, 1234–1245.

Declarations

Funding

The author declared no external sources kf funding

Conflict of Interest

The author declared no conflict of interest

Data Availability

Data shall be made available upon request

Ethical Considerations

Not applicable

Authors; Contributions

The authors contributed to the conceptualization and design of the study, synthesis and characterization of the CdO–Fe_2O_3 nanocomposite, electrochemical sensing experiments, antifungal evaluation, data analysis, interpretation of results, and manuscript preparation. All authors reviewed the manuscript, provided intellectual input, and approved the final version for publication.